Eur. Phys. J. C 35, 177–187 (2004)
Digital Object Identifier (DOI) 10.1140/epjc/s2004-01812-7

THE EUROPEAN PHYSICAL JOURNAL C

Dynamical selection rules from $p\bar{p}$ annihilation at rest in three meson final states

The OBELIX Collaboration

M. Bargiotti[1], A. Bertin[1], M. Bruschi[1], M. Capponi[1], A. Carbone[1], S. De Castro[1], R. Donà[1], L. Fabbri[1], P. Faccioli[1], D. Galli[1], B. Giacobbe[1], F. Grimaldi[1], U. Marconi[1], I. Massa[1], M. Piccinini[1], N. Semprini Cesari[1], R. Spighi[1], S. Vecchi[1], M. Villa[1], A. Vitale[1], A. Zoccoli[1], M. Poli[2], A. Bianconi[3], M.P. Bussa[3], M. Corradini[3], A. Donzella[3], E. Lodi Rizzini[3], L. Venturelli[3], C. Cicalò[4], A. De Falco[4], A. Masoni[4], G. Puddu[4], S. Serci[4], G. Usai[4], O.E. Gorchakov[5], S.N. Prakhov[5], A.M. Rozhdestvensky[5], M.G. Sapozhnikov[5], V.I. Tretyak[5], P. Gianotti[6], C. Guaraldo[6], A. Lanaro[6], V. Lucherini[6], C. Petrascu[6], R. A. Ricci[7], V. Filippini[8], A. Fontana[8], P. Montagna[8], A. Panzarasa[9], A. Rotondi[8], P. Salvini[8], A. Zenoni[3], F. Balestra[10], L. Busso[10], P. Cerello[10], O. Denisov[10], L. Ferrero[10], R. Garfagnini[10], A. Maggiora[10], D. Panzieri[14], F. Tosello[10], E. Botta[11], T. Bressani[11], D. Calvo[11], F. De Mori[11], A. Feliciello[11], A. Filippi[11], N. Mirfakhrai[12], S. Marcello[11], M. Agnello[13], F. Iazzi[13].

[1] Dipartimento di Fisica dell'Università di Bologna and INFN Sezione di Bologna, Bologna, Italy
[2] Dipartimento di Energetica dell'Università di Firenze, Firenze, Italy and INFN Sezione di Bologna, Bologna, Italy
[3] Dipartimento di Chimica e Fisica per l'Ingegneria e per i Materiali, Università di Brescia, Brescia, Italy and INFN gruppo collegato di Brescia, Brescia, Italy
[4] Dipartimento di Scienze Fisiche, Università di Cagliari and INFN Sezione di Cagliari, Cagliari, Italy
[5] Joint Institute for Nuclear Research, Dubna, Russia
[6] Lab. Naz. di Frascati dell'INFN, Frascati, Italy
[7] Lab. Naz. di Legnaro dell'INFN, Legnaro, Italy
[8] Dipartimento di Fisica Nucleare e Teorica dell'Università di Pavia and INFN Sezione di Pavia, Pavia, Italy
[9] INFN Sezione di Pavia, Pavia, Italy
[10] Dipartimento di Fisica Generale dell'Università di Torino and INFN Sezione di Torino, Torino, Italy
[11] Dipartimento di Fisica Sperimentale dell'Università di Torino and INFN Sezione di Torino, Torino, Italy
[12] Shahid Behesty University, Teheran, Iran
[13] Dipartimento di Fisica del Politecnico di Torino and INFN Sezione di Torino, Torino, Italy
[14] Universita' del Piemonte Orientale e INFN, Sezione di Torino, Torino, Italy

Received: 4 February 2004 /
Published online: 5 May 2004 –

Abstract. The hadronic annihilation branching-ratios in quasi-two-body final states have been obtained from the observation of the reactions $\bar{p}p \to \pi^+\pi^-\pi^0$, $K^+K^-\pi^0, K^\pm\pi^\mp K^0$ at rest in hydrogen targets at different densities. The enhancement or suppression of specific hadronic channels connected to dynamical selection rules is observed in the production of different resonances both in protonium S and P–waves, systematically investigated for the first time. Besides the well known $\rho(770)\pi$ and $a_2(1320)\pi$ enhancement from $^3S_1$ and $^1S_0$ partial waves, the dominance of one isospin source in $K^*(892)\bar{K}$ production, well established from S–waves, is confirmed also in P–waves ($^1S_0$, $I=0$; $^3S_1$, $I=1$; $^1P_1$, $I=0$; $^3P_1$, $I=0$; $^3P_2$, $I=1$). In addition, the experimental data clearly show a strong suppression of $\phi(1020)\pi$ and $a_0(980)\pi$ final states from P–wave which has a remarkable coincidence with $K^*(892)\bar{K}$ pattern production.

1 Introduction

Most of the meson decay phenomenology can be described correctly by means of the so called quark line rule [1]. Initially suggested as a purely empirical law and now understood, to some extent, within the framework of QCD, it explains for instance the small width of the J/ψ or why the ϕ meson decays preferentially in $K\bar{K}$. The success of the quark line rule has suggested the search of equivalent prescriptions at the quark level also in $N\bar{N}$ annihilation [2].

In many cases in fact, the measurements of $N\bar{N}$ annihilation branching ratios in two body and quasi two body (where quasi means resonant) final states show a strong departure from the statistical behaviour, consisting in the suppression of specific channels allowed by the conservation laws (in spite of the success of statistical models in explaining some general features of $N\bar{N}$ annihilation like

meson multiplicities, momentum distributions, etc.). The occurrence of such a suppression represents the clearest experimental indication that dynamical selection rules operate also in the annihilation process.

Even so, the extraction of the underlying quark dynamics from these annihilation branching ratios is a delicate issue since also $N\bar{N}$ initial and final state interactions (scattering) can modify the relative intensity of the different annihilation channels. For these reasons the effectiveness of this study relies on the availability of sets of branching ratios relative to the different quantum numbers of the $N\bar{N}$ system (isospin and angular momentum) and involving final state mesons of different spin and flavour composition.

At present most of the available measurements come from $p\bar{p}$ annihilation at rest in hydrogen targets. Annihilations proceed from both the isospin $I = 0$ and $I = 1$ and from two S–waves ($^1S_0$ and $^3S_1$) and four P–waves ($^1P_1$, $^3P_0$,$^3P_1$ and $^3P_2$) with strength which depends on the target density (see the description of the protonium atom deexcitation in [3] and references therein). While S–wave dynamics has been explored by means of systematic measurements in liquid hydrogen targets (where the S–wave contribution is dominant) our knowledge of P–wave dynamics is still unsatisfactory. This is due both to the fact that a smaller amount of experimental data from gaseous hydrogen targets (where the P–wave contribution is considerable) are available and to the fact that at least four partial waves are usually involved.

This fact suggested us to extract from the coupled channel analysis of the reactions $p\bar{p} \to \pi^+\pi^-\pi^0$, $K^+K^-\pi^0$ and $K^\pm K^0\pi^\mp$, performed at three different densities of the hydrogen targets [3], the dominant quasi two body (QTB in the following) branching ratios both from all S and P partial waves.

Concerning these data, mainly two aspects have to be underlined. First $K\bar{K}\pi$ final state has been observed in two different isospin configurations in order to guarantee a reliable control on the complex $K\pi$ and $K\bar{K}$ dynamics. Second, each final state was observed in hydrogen targets of different densities. This technique, developed and systematically employed for the first time by the OBELIX experiment, is based on a series of density dependent mechanisms involving the protonium atom in the hydrogen medium ([3] and references therein) which lead to dominant S–wave annihilation in the case of liquid hydrogen (LH), dominant P–wave in low density hydrogen (LP) and comparable fractions of S and P–wave in normal density (NP) hydrogen. In this way a reliable control over the different partial waves contributing to $p\bar{p}$ annihilation at rest is obtained.

The analysis described in this paper is mainly focused on the resonances which dominate the decay channels accessible to the available three meson final states $f_0(980)\pi$, $a_0(980)\pi$, $\phi(1020)\pi$, $K^*(892)\bar{K}$, $\rho(770)\pi$, $f_2(1270)\pi$, $f_2'(1525)\pi$ and $a_2(1320)\pi$. The details concerning the QTB branching ratio calculations and the analysis of the corresponding experimental data are described in Sect. 2; Sects. 3 and 4 are devoted to the discussion of the results, and Sect. 5 to the conclusions.

2 Data analysis

The starting point of the present analysis is represented by the QTB fractions from all S and P partial waves of $p\bar{p}$ system measured in the coupled-channel analysis of $p\bar{p}$ annihilation in $\pi^+\pi^-\pi^0$, $K^+K^-\pi^0$ and $K^\pm K^0\pi^\mp$ at three different target densities (for details see Table 3 of [3] and comments therein). In this analysis we add an interesting piece of information represented by $K^*(892)\bar{K}$ fractions from each of the isospin sources ($I = 0, 1$) of the $p\bar{p}$ system.

In order to get the QTB annihilation branching ratios these fractions have been divided by the inverse squared of the appropriate isospin coefficients and resonance decay branching ratios (assumed by the PDG [5] except for the $f_0(980)$ resonance where the values [3] are used).

The central values of QTB annihilation branching ratios are obtained by averaging a set of values corresponding to coupled–channels analysis fits with good χ^2. From the same set we evaluate also the associated systematic errors which are expected to dominate the overall uncertainties. The results are shown in Table 1 where the QTB annihilation branching ratios from each S and P partial wave and isospin source involved in $p\bar{p}$ annihilation at rest at different hydrogen densities are listed. Any deviations from the values calculated using the values of [3], which correspond to the best fit solution, are due to the averaging procedure.

In the QTB annihilation branching ratios the hadronic part of the process we are interested in depends on the atomic physics involved in the $p\bar{p}$ system. Indicating by $BR_j^k(\rho)$ the QTB annihilation branching ratio at the density ρ from the partial wave k in the final state j, by $\mathcal{BR}_j^k$ the hadronic QTB annihilation branching ratio and by $W^k(\rho)$ the fraction of the partial wave k at the density ρ, we get the following equation:

$$BR_j^k(\rho) \;=\; W^k(\rho)\,\mathcal{BR}_j^k \;=\; f_{S,P}(\rho)\,S^k\,E^k(\rho)\,\mathcal{BR}_j^k \qquad (1)$$

In the last equality the coefficients $W^k(\rho)$ are expressed in the notation of [6], where $f_{S,P}(\rho)$ represents S or P–wave fraction ($f_S = 1 - f_P$), S^k the statistical weight of the k^{th} partial wave ($^1S_0 = 1/4$, $^3S_1 = 3/4$, $^1P_1 = 3/12$, $^3P_0 = 1/12$, $^3P_1 = 3/12$, $^3P_2 = 5/12$) and $E^k(\rho)$ the enhancement factors which describe possible deviations from the statistical distribution S^k.

In order to extract the hadronic branching ratios $\mathcal{BR}_j^k$ the P–wave fractions $f_P(\rho)$ and the enhancement factors $E^k(\rho)$ have to be evaluated first. To this aim we fit a rich set of experimental data including two, three, and four mesons $p\bar{p}$ annihilation branching ratios in different experimental conditions (Table 2).

As far as these data are concerned, the following remarks are necessary. The two meson $p\bar{p}$ annihilation at rest usually occurs from two or three different partial waves with the exception of the $\phi\pi$ and K_SK_L final states, were only the $^3S_1$ level is involved. Annihilation in $\pi^+\pi^-\pi^0$, $K^+K^-\pi^0$ and $K^\pm K^0\pi^\mp$ final states takes place from five different partial waves ($^1S_0$, $^3S_1$, $^1P_1$, $^3P_1$ and $^3P_2$ while $^3P_0$ is forbidden by selection rules) but, contrarly to two mesons, through a partial wave analysis the contribution of each

Table 1. Quasi two body annihilation branching ratios from $p\bar{p}$ annihilation at rest at different densities (units of 10^{-3})

Channel	*PW*			*LH*	*NP*	*LP*	*Final State*
$f_0(980)\pi$	$^1S_0$			0.49 ± 0.16	0.27 ± 0.09	0.13 ± 0.04	$\pi^+\pi^-\pi^0$
	$^3P_1$			0.12 ± 0.04	0.28 ± 0.10	0.40 ± 0.15	
		Total		0.6 ± 0.2	0.54 ± 0.19	0.52 ± 0.19	
	$^1S_0$			0.46 ± 0.17	0.27 ± 0.10	0.12 ± 0.05	$K^+K^-\pi^0$
	$^3P_1$			0.10 ± 0.04	0.27 ± 0.10	0.37 ± 0.14	
		Total		0.6 ± 0.2	0.5 ± 0.2	0.49 ± 0.18	
$a_0(980)\pi$	$^1S_0$			3.0 ± 0.3	1.75 ± 0.17	0.78 ± 0.06	$K^+K^-\pi^0$
	$^3P_1$			0.04 ± 0.02	0.10 ± 0.06	0.13 ± 0.08	
		Total		3.0 ± 0.5	1.9 ± 0.2	0.91 ± 0.14	
	$^1S_0$			2.9 ± 0.4	1.16 ± 0.17	0.54 ± 0.08	$K^\pm K^0\pi^\mp$
	$^1P_1$			$< 10^{-3}$	0.014 ± 0.008	0.02 ± 0.01	
	$^3P_1$			0.04 ± 0.02	0.07 ± 0.04	0.10 ± 0.06	
		Total		2.9 ± 0.5	1.2 ± 0.2	0.66 ± 0.15	
$\phi(1020)\pi$	$^3S_1$			0.50 ± 0.08	0.29 ± 0.05	0.13 ± 0.02	$K^+K^-\pi^0$
	$^1P_1$			$< 10^{-2}$	$< 10^{-2}$	$< 10^{-2}$	
$K^*(892)\bar{K}$	$^1S_0$	$I=0$		0.90 ± 0.11	0.53 ± 0.07	0.23 ± 0.03	$K^+K^-\pi^0$
		$I=1$		0.26 ± 0.07	0.15 ± 0.04	0.067 ± 0.017	
	$^3S_1$	$I=0$		0.28 ± 0.05	0.16 ± 0.03	0.072 ± 0.011	
		$I=1$		2.03 ± 0.14	1.19 ± 0.08	0.53 ± 0.04	
	$^1P_1$	$I=0$	$L=0$	0.007 ± 0.002	0.96 ± 0.07	1.3 ± 0.10	
			$L=2$	0.0006 ± 0.0007	0.08 ± 0.08	0.11 ± 0.11	
		$I=1$	$L=0$	0.00046 ± 0.00017	0.067 ± 0.015	0.09 ± 0.02	
			$L=2$	0.0016 ± 0.0005	0.23 ± 0.02	0.31 ± 0.03	
	$^3P_1$	$I=0$	$L=0$	0.48 ± 0.05	1.23 ± 0.13	1.67 ± 0.18	
			$L=2$	0.43 ± 0.04	1.09 ± 0.01	1.48 ± 0.14	
		$I=1$	$L=0$	0.012 ± 0.005	0.03 ± 0.01	0.042 ± 0.016	
			$L=2$	0.085 ± 0.007	0.217 ± 0.018	0.29 ± 0.03	
	$^3P_2$	$I=0$		0.150 ± 0.014	0.38 ± 0.03	0.52 ± 0.05	
		$I=1$		0.81 ± 0.06	2.06 ± 0.15	2.8 ± 0.2	
		Total		6.3 ± 0.4	9.0 ± 0.6	9.9 ± 0.7	
	$^1S_0$	$I=0$		0.90 ± 0.14	0.37 ± 0.07	0.17 ± 0.03	$K^\pm K^0\pi^\mp$
		$I=1$		0.20 ± 0.06	0.08 ± 0.02	0.038 ± 0.009	
	$^3S_1$	$I=0$		0.29 ± 0.06	0.12 ± 0.02	0.055 ± 0.010	
		$I=1$		1.6 ± 0.2	0.64 ± 0.09	0.30 ± 0.05	
	$^1P_1$	$I=0$	$L=0$	0.007 ± 0.002	0.68 ± 0.10	0.98 ± 0.14	
			$L=2$	0.0006 ± 0.0007	0.06 ± 0.05	0.08 ± 0.08	
		$I=1$	$L=0$	0.0005 ± 0.0002	0.051 ± 0.014	0.07 ± 0.02	
			$L=2$	0.0015 ± 0.0005	0.16 ± 0.02	0.22 ± 0.03	
	$^3P_1$	$I=0$	$L=0$	0.49 ± 0.08	0.87 ± 0.14	1.2 ± 0.2	
			$L=2$	0.43 ± 0.06	0.76 ± 0.11	1.08 ± 0.16	
		$I=1$	$L=0$	0.012 ± 0.004	0.021 ± 0.008	0.029 ± 0.011	
			$L=2$	0.088 ± 0.012	0.16 ± 0.02	0.22 ± 0.03	
	$^3P_2$	$I=0$		0.15 ± 0.02	0.27 ± 0.04	0.39 ± 0.06	
		$I=1$		0.69 ± 0.09	1.23 ± 0.18	1.8 ± 0.3	
		Total		4.8 ± 0.6	5.3 ± 0.7	6.4 ± 0.9	
$\rho(770)\pi$	$^1S_0$			1.4 ± 0.3	0.77 ± 0.15	0.36 ± 0.05	$\pi^+\pi^-\pi^0$
	$^3S_1$			49 ± 3	26 ± 2	9.6 ± 1.0	
	$^1P_1$		$L=0$	0.01 ± 0.01	0.5 ± 0.3	0.7 ± 0.5	
			$L=2$	0.3 ± 0.3	7 ± 1	10.6 ± 1.0	
	$^3P_1$		$L=0$	2.4 ± 0.4	5.8 ± 1.2	8 ± 2	
			$L=2$	0.03 ± 0.04	0.06 ± 0.09	0.09 ± 0.12	
	$^3P_2$			0.95 ± 0.2	2.3 ± 0.6	3.3 ± 0.9	
		Total		54 ± 3	43 ± 3	33 ± 2	

Table 1. (continued)

Channel	*PW*	*LH*	*NP*	*LP*	*Final State*
$f_2(1270)\pi$	$^1S_0$	2.7 ± 0.2	1.5 ± 0.7	0.7 ± 0.4	$\pi^+\pi^-\pi^0$
	$^3P_1$	3.0 ± 0.4	7 ± 4	10 ± 6	
	$^3P_2$	0.88 ± 0.07	2.1 ± 1.0	3.0 ± 1.7	
	Total	6.6 ± 0.7	10.6 ± 1.1	13.9 ± 1.4	
	$^1S_0$	2.6 ± 0.8	1.5 ± 0.4	0.7 ± 0.2	$K^+K^-\pi^0$
	$^3P_1$	3.0 ± 0.6	7.6 ± 1.7	10 ± 2	
	$^3P_2$	0.90 ± 0.2	2.3 ± 0.6	3.1 ± 0.8	
	Total	6.5 ± 1.7	11 ± 3	14 ± 4	
$f_2'(1525)\pi$	$^1S_0$	0.10 ± 0.02	0.056 ± 0.012	0.025 ± 0.006	$K^+K^-\pi^0$
	$^3P_1$	0.078 ± 0.008	0.20 ± 0.02	0.27 ± 0.03	
	$^3P_2$	0.05 ± 0.02	0.11 ± 0.05	0.16 ± 0.06	
	Total	0.22 ± 0.02	0.37 ± 0.05	0.45 ± 0.08	
$a_2(1320)\pi$	$^1S_0$	12.2 ± 1.8	7.1 ± 1.0	3.2 ± 0.4	$K^+K^-\pi^0$
	$^3P_1$	0.18 ± 0.15	0.5 ± 0.4	0.6 ± 0.5	
	$^3P_2$	0.5 ± 0.1	1.3 ± 0.3	1.7 ± 0.4	
	Total	13 ± 3	8.9 ± 1.9	5.5 ± 1.1	
	$^1S_0$	12 ± 2	5.0 ± 0.9	2.3 ± 0.4	$K^\pm K^0\pi^\mp$
	$^3S_1$	3.3 ± 0.5	1.3 ± 0.2	0.6 ± 0.1	
	$^1P_1$	0.03 ± 0.01	3.2 ± 0.4	4.5 ± 0.6	
	$^3P_1$	0.19 ± 0.15	0.3 ± 0.2	0.5 ± 0.4	
	$^3P_2$	0.51 ± 0.14	0.9 ± 0.3	1.3 ± 0.4	
	Total	16 ± 4	11 ± 2	9 ± 2	

level can be evaluated separately. The same considerations hold in the case of $\eta(1440)\pi^+\pi^-$, produced from the $^1S_0$ level, and the $\pi^+\pi^-\pi^+\pi^-$ final state, which occurs from all S and P partial waves. The partial wave analysis of this channel provides, besides, the only annihilation branching ratio from *"pure"* $^3P_0$ level so far available. A crucial part of this approach relies on the availability of these branching ratios in hydrogen targets of different densities since changes in branching ratios are due only to the atomic part of the process i.e. the coefficients $f_P(\rho)$ and $E^k(\rho)$ (see (1)).

The data were fitted by minimizing the chi-square function and by requiring the following additional conditions: (i) $\pi^+\pi^-$ and K^+K^- measurements with X-rays coincidence were assumed as coming from pure P–waves; (ii) $\pi^+\pi^-\pi^+\pi^-$ branching ratios measured in gaseous hydrogen at 3 *bar* were treated as NP data; (iii) $\pi^0\pi^0$, $\pi^0\eta$ and $\eta\eta$ branching ratios in liquid hydrogen were excluded from the fit (see Table 2). Concerning the hyperfine levels the following different assumptions were done:

(a) statistical distribution, imposed by fixing $E^k(\rho) = 1$. The poor $\chi^2/ndf = 5.5$ obtained shows that the data are not compatible with this hypothesis;
(b) enhancement factors fixed to the values derived from cascade and $\bar{N}N$ potential models [6] (Table 3). Also in this case the agreement is unsatisfactory ($\chi^2/ndf = 5.02$) expecially for the LH $^1P_1$ and $^3P_1$ data from spin-parity analyses;
(c) Free enhancement factors. In this case we get a very good description of the data, with $\chi^2/ndf \sim 1.25$, but several solutions with different enhancement factors are found with similar χ^2. This instability, already experienced in previous analyses [24], is due to the non–linearity of the problem and seems not to be solved;
(d) To get results unaffected by stability problems we assumed, like in [24], a statistical distribution of the fine structure levels at low pressure hydrogen ($E^k(LP) = 1$). This hypothesis is also supported by the prediction of the cascade model [6]. A good solution, wihout ambiguities, is found with $\chi^2/ndf = 1.34$.

The values of the enhancement factors and P–wave fractions found by the last hypothesis are reported in Table 3. For comparison we report also the values corresponding to the assumption (b). As expected, the P–wave fractions are controlled by the hydrogen density, nevertheless the f_P values obtained show clearly that the P–wave contribution cannot be neglected even in liquid hydrogen. Enhancement factors different from one are observed above all in liquid hydrogen from $^1P_1$, $^3P_0$ and $^3P_1$ levels. The comparison with the model predictions [6] shows a good agrement for the $^3P_0$ level, but a strong disagreement for the other levels. In particular the $^1P_1$ suppression in LH, strongly requested by the spin-parity analysis data, is not explained by any cascade model and has never been requested by previous analyses of two meson branching ratios. This result is found in $\pi^+\pi^-\pi^+\pi^-$ spin–parity analysis (see Table 4 of [22]) and even more evident in the coupled–channel analysis [3].

To get an insight into the controversial problem of the $\pi^0\pi^0$ branching ratio in liquid hydrogen, using the fit parameters we can calculate the expected value $(0.49\pm0.05)\times 10^{-3}$ to be compared to the ones listed in Table 2.

Following equation (1) and given the $f_{S,P}(\rho)$ and $E^k(\rho)$ values listed in Table 3, the QTB hadronic branching ratios

Table 2. Branching ratios into two, three and four mesons from $p\bar{p}$ annihilation at rest at different densities (units of 10^{-3}). (AV): average over the existing measurements (see [7]). (†): measurement made requiring the X-ray coincidence. (*): hydrogen density corresponding to a target pressure of 3 bar

Channel		*LH*	Ref.	*NP*	Ref.	*LP*	Ref.
$\pi^+\pi^-$		3.11 ± 0.11	AV	4.29 ± 0.12	AV	4.26 ± 0.11	[8]
						4.8 ± 0.5 †	[9]
$\pi^0\pi^0$		0.28 ± 0.04	[10]	1.3 ± 0.2	[11]		
		0.69 ± 0.04	[12]				
$\pi^0\eta$		0.09 ± 0.02	[13]	0.34 ± 0.07	[14]		
		0.212 ± 0.012	[15]				
$\eta\eta$		0.08 ± 0.03	[16]	0.27 ± 0.07	[14]		
		0.164 ± 0.014	[17]				
K^+K^-		0.992 ± 0.017	AV	0.69 ± 0.04	[9]	0.46 ± 0.03	[8]
						0.29 ± 0.05 †	[9]
K_SK_L		0.78 ± 0.03	AV	0.36 ± 0.04	AV	0.10 ± 0.03	[18]
						0.07 ± 0.06 †	[19]
K_SK_S		0.004 ± 0.003	AV	0.03 ± 0.01	[19]	0.037 ± 0.014	[19]
$\phi\pi^0$		0.50 ± 0.03	AV	0.233 ± 0.013	AV	0.092 ± 0.010	[21]
$\pi^+\pi^-\pi^0$	$^1S_0$	9.4 ± 0.7	[3]	4.9 ± 0.4	[3]	2.1 ± 0.5	[3]
	$^3S_1$	36 ± 2	[3]	18.5 ± 1.1	[3]	7.9 ± 0.8	[3]
	$^1P_1$	0.05 ± 0.38	[3]	9.9 ± 0.8	[3]	13.6 ± 1.3	[3]
	$^3P_1$	5.5 ± 0.7	[3]	12.0 ± 1.0	[3]	16.5 ± 1.3	[3]
	$^3P_2$	2.9 ± 0.3	[3]	6.3 ± 0.7	[3]	8.7 ± 1.1	[3]
	Total	53.6 ± 2.7	[21]	51.6 ± 2.6	[21]	48.9 ± 2.8	[21]
$K^+K^-\pi^0$	$^1S_0$	0.90 ± 0.07	[3]	0.52 ± 0.05	[3]	0.22 ± 0.04	[3]
	$^3S_1$	0.89 ± 0.08	[3]	0.52 ± 0.04	[3]	0.22 ± 0.02	[3]
	$^1P_1$	0.002 ± 0.02	[3]	0.57 ± 0.08	[3]	0.78 ± 0.12	[3]
	$^3P_1$	0.41 ± 0.05	[3]	1.01 ± 0.09	[3]	1.38 ± 0.14	[3]
	$^3P_2$	0.16 ± 0.05	[3]	0.40 ± 0.12	[3]	0.55 ± 0.16	[3]
	Total	2.37 ± 0.16	[21]	3.03 ± 0.20	[21]	3.15 ± 0.22	[21]
$K^\pm K^0_S\pi^\mp$	$^1S_0$	1.12 ± 0.18	[3]	0.45 ± 0.07	[3]	0.20 ± 0.04	[3]
	$^3S_1$	1.09 ± 0.18	[3]	0.43 ± 0.06	[3]	0.19 ± 0.03	[3]
	$^1P_1$	0.006 ± 0.05	[3]	1.2 ± 0.2	[3]	1.7 ± 0.3	[3]
	$^3P_1$	0.60 ± 0.12	[3]	1.02 ± 0.17	[3]	1.5 ± 0.3	[3]
	$^3P_2$	0.35 ± 0.08	[3]	0.59 ± 0.13	[3]	0.84 ± 0.19	[3]
	Total	3.16 ± 0.40	[35]	3.64 ± 0.50	[35]	4.32 ± 0.60	[35]
$\eta(1440)\pi^+\pi^-$		0.63 ± 0.04	AV	0.29 ± 0.04	AV	0.10 ± 0.02	[20]
$\pi^+\pi^-\pi^+\pi^-$	$^1S_0$	10.9 ± 0.5	[22]	5.40 ± 0.13 *	[22]		
	$^3S_1$	32.4 ± 1.4	[22]	18 ± 3 *	[22]		
	$^1P_1$	0.5 ± 0.3	[22]	3.9 ± 0.6 *	[22]		
	$^3P_0$	6.9 ± 0.5	[22]	9.7 ± 1.4 *	[22]		
	$^3P_1$	2.6 ± 0.3	[22]	3.3 ± 0.6 *	[22]		
	$^3P_2$	6.7 ± 0.5	[22]	24 ± 3 *	[22]		
	Total	60.0 ± 2.4	[22]	64 ± 9 *	[23]		

Table 3. Chisquare, enhancement factors $E^k(\rho)$ and P–wave fractions $f_P(\rho)$ obtained by fitting the $p\bar{p}$ annihilation branching ratios into two, three and four mesons of Table 2 according to different assumptions: first block: fit **b** (enhancement factors given by [6] (DR1 model)); second block: fit **d** (enhancement factors at low pressure fixed to one). The quoted errors are estimated by the minimization program MINUIT

Density	f_P	$E^{^1S_0}$	$E^{^3S_1}$	$E^{^1P_1}$	$E^{^3P_0}$	$E^{^3P_1}$	$E^{^3P_2}$
LH	0.19 ± 0.02	1.032	0.989	0.856	2.556	0.685	0.964
NP	0.60 ± 0.01	1.020	0.993	0.974	1.288	0.929	1.000
LP	0.83 ± 0.01	1.046	0.985	0.999	1.016	0.993	1.002
							$\chi^2/ndf = 5.02$
LH	0.20 ± 0.02	1.23 ± 0.03	0.92 ± 0.01	0.09 ± 0.17	2.15 ± 0.50	1.44 ± 0.26	1.05 ± 0.04
NP	0.60 ± 0.02	1.19 ± 0.06	0.94 ± 0.02	0.87 ± 0.04	0.97 ± 0.40	0.96 ± 0.20	1.11 ± 0.04
LP	0.84 ± 0.01	1	1	1	1	1	1
							$\chi^2/ndf = 1.34$

Table 4. Hadronic branching-ratios of $\bar{p}p$ annihilation in quasi two body final states (units of 10^{-3}). See text for the details

Channel		$^1S_0$	$^3S_1$	$^1P_1$		$^3P_1$		$^3P_2$
$f_0(980)\pi$		2.3 ± 0.3				1.7 ± 0.3		
$a_0(980)\pi$		12.9 ± 0.9		0.05 ± 0.08		0.51 ± 0.14		
$\phi(1020)\pi$			1.00 ± 0.09	$< 10^{-2}$				
$K^*(892)\bar{K}$	I=0	4.0 ± 0.3	0.51 ± 0.04	6.0 ± 0.3	$L=0$	7.0 ± 0.5	$L=0$	1.34 ± 0.06
				0.07 ± 0.07	$L=2$	6.2 ± 0.4	$L=2$	
	I=1, $K^+K^-\pi^0$	1.3 ± 0.2	4.0 ± 0.2	0.45 ± 0.08	$L=0$	0.19 ± 0.05	$L=0$	7.9 ± 0.4
				1.59 ± 0.12	$L=2$	1.4 ± 0.1	$L=2$	
	I=1, $K^\pm K^0\pi^\mp$	0.81 ± 0.13	2.5 ± 0.2	0.35 ± 0.07	$L=0$	0.14 ± 0.03	$L=0$	5.2 ± 0.5
				1.09 ± 0.12	$L=2$	1.07 ± 0.12	$L=2$	
$\rho(770)\pi$		7.0 ± 0.8	89 ± 4	2.2 ± 2.1	$L=0$	37 ± 6	$L=0$	9.3 ± 1.4
				50 ± 4	$L=2$	0.41 ± 0.34	$L=2$	
$f_2(1270)\pi$		12.1 ± 0.7				47 ± 4		8.4 ± 0.5
$f_2'(1525)\pi$		0.45 ± 0.06				1.27 ± 0.12		0.44 ± 0.11
$a_2(1320)\pi$		53 ± 5	5.3 ± 0.7	22 ± 4		2.5 ± 0.9		4.3 ± 0.6

$\mathcal{BR}_j^k$ can be extracted from the measured QTB annihilation branching ratios $BR_j^k(\rho)$ of Table 1 by means of a fitting procedure. In order to take properly into account the $W^k(\rho)$ errors due to the $f_{S,P}(\rho)$ and $E^k(\rho)$ uncertainties, the following log-likelihood function was minimized:

$$-2\ln\mathcal{L} = \sum_{k,j,\rho} \frac{(BR_j^k(\rho) - W^k(\rho)\mathcal{BR}_j^k)^2}{\delta BR_j^k(\rho)^2 + \delta W^k(\rho)^2 \mathcal{BR}_j^{k\,2}} + \sum_{k,j,\rho} \ln(\delta BR_j^k(\rho)^2 + \delta W^k(\rho)^2 \mathcal{BR}_j^{k\,2}) + cost.$$

The results obtained are listed in Table 4 ($\chi^2/ndf = 0.74$), will be presented in the next Section.

3 Main results

$f_0(980)\pi$. Due to closeness to $K\bar{K}$ threshold, and to the underlying non-resonant background, the $f_0(980)$ physical state turns out to be strongly distorted. For this reason we decided to calculate the QTB branching ratios approximating the physical state by a Breit Wigner function [4]. The values obtained from $\pi^+\pi^-\pi^0$ and $K^+K^-\pi^0$ final states are in very good agreement (see Table 1).

$a_0(980)\pi$. The values of $a_0(980)\pi$ QTB branching ratios listed in Table 1 are obtained assuming the $\Gamma(K\bar{K})/\,\Gamma(\eta\pi)$ mean value quoted by PDG [5] by neglecting all the other decay modes (in this way we get $\Gamma(K\bar{K})/\,\Gamma_{Tot} = 0.15 \pm 0.02$ and $\Gamma(\eta\pi)/\,\Gamma_{Tot} = 0.85 \pm 0.02$). The present liquid hydrogen measurement can be compared to the previous determination in $\pi^0\pi^0\eta$ final state $(2.9\pm0.7)\times10^{-3}$ [26] and in $K^\pm K_L^0\pi^\mp$ final state $(3.94^{+0.30}_{-0.68}) \times 10^{-3}$ [27] obtaining a satisfactory agreement. The measurements at different densities can be compared only to the previous OBELIX determinations in $K^\pm K_S^0\pi^\mp$ final state (LH: $(2.96\pm0.60)\times10^{-3}$; NP: $(1.49\pm0.25)\times10^{-3}$; LP: $(0.52\pm0.13)\times10^{-3}$) [35] which are also compatible within the experimental errors.

The coupled channel analysis [3] shows clearly that the $a_0(980)\,\pi$ production from the P–waves of $p\bar{p}$ system, even if allowed by selection rules, is suppressed with respect to S–wave (see Tables 1 and 4). This fact, previously observed in [35], is also suggested by the direct inspection of the experimental data. In fact, as shown in [3] and [35] lowering the hydrogen density, i.e. increasing the P–wave contribution, leads to the suppression of the $a_0(980)$ peak in the $K^\pm K^0\pi^\mp$ final state. At present the origin of this dynamical selection rule remains unexplained.

$\phi(1020)\pi$. It is well known that the $\phi(1020)$ production in $\bar{N}N$ annihilation exceeds largely the predictions of the so called OZI-rule, a decay scheme which has successfully explained the properties of many mesons and now is included in the framework of QCD [1]. In the case of the $\phi(1020)\pi$ final state, the measured branching ratios (listed in Table 1) lead to a violation of OZI-rule predictions by a factor of 20–50 [28]. The listed values are affected by relatively large errors due to the fact that the binning of $K^+K^-\pi^0$ Dalitz-plots was chosen to perform the spin-parity analysis, and was not optimized to resolve the $\phi(1020)$ peak. Reminding this fact, our liquid hydrogen measurement can be compared to the value $(65 \pm 6) \times 10^{-5}$ quoted in [31] and to $(48.8 \pm 3.2) \times 10^{-5}$ of [21]; NP hydrogen measurement to $(19 \pm 5) \times 10^{-5}$ [32], $(24.6 \pm 3.0) \times 10^{-5}$ [34] and $(24.7 \pm 2.1) \times 10^{-5}$ [21]; and finally LP hydrogen measurement to $(9.2 \pm 1.0) \times 10^{-5}$ obtained in [21]. As in the $a_0(980)$ case, the spin-parity analysis of the $K^+K^-\pi^0$ final state shows that the large $\phi(1020)\pi$ production comes, almost completely, from $^3S_1$ even though also the $^1P_1$ partial wave would be allowed by selection rules (see Tables 1 and 4). This feature of $\phi(1020)\pi$ production, directly exhibited by the experimental data (the same comments done in the case of $a_0(980)\pi$ are valid), at present is unexplained.

$K^*(892)\bar{K}$. As far as $K^*(892)\bar{K}$ QTB branching ratios are concerned some specifications are necessary. This channel has not a defined G–parity so that each $\bar{p}p$ partial wave contributes to the annihilation with both the $I = 0$ and

$I = 1$ components coherently. This means that the total $K^*(892)\bar{K}$ branching ratio includes the $I = 0$ and $I = 1$ interference effect in each partial wave which, on the contrary, are excluded in the individual branching ratio evaluation. For this reason the $I = 0$ and $I = 1$ QTB branching ratios listed in Table 1 cannot be summed to get the total $K^*(892)\bar{K}$ branching ratio. Moreover the $K^*(892)\bar{K}$ interference depends on the final state, and therefore its branching ratio too. The total branching ratios quoted in Table 1 are calculated following these considerations.

The $K^*(892)\bar{K}$ channel branching ratios at different densities was previously measured by OBELIX in the $K^+K^-\pi^0$ final state (LH: $(5.2 \pm 0.9) \times 10^{-3}$; NP: $(7.0 \pm 0.8) \times 10^{-3}$; LP: $(7.4 \pm 0.9) \times 10^{-3}$) [21] and $K^\pm K^0\pi^\mp$ final state (LH: $(4.6 \pm 0.6) \times 10^{-3}$; NP: $(5.1 \pm 0.5) \times 10^{-3}$; LP: $(6.0 \pm 0.8) \times 10^{-3}$) [35]; and in LH by CRYSTAL BARREL $(4.2 \pm 0.3) \times 10^{-3}$ [36]. These values agree, within the experimental errors, with the determinations reported in Table 1.

The $\bar{p}p$ annihilation in $K^*(892)\bar{K}$ from S–wave exhibits a very interesting dynamical selection rule consisting in the suppression of one of the two allowed isospin components i.e. $I = 1$ in the $^1S_0$ partial wave and $I = 0$ in the $^3S_1$ partial wave. This result, obtained first in bubble chamber experiments [37], and by CRYSTAL BARREL [38] in the $K^\pm K^0\pi^\mp$ final state, is also confirmed by the present analysis (the ratios, calculated by means of the QTB hadronic branching ratios, are indicated by [*]):

$$^1S_0 \; : \; \frac{BR(p\bar{p} \to K^*(892)\bar{K})_{I=1}}{BR(p\bar{p} \to K^*(892)\bar{K})_{I=0}} \; = \; \begin{cases} 0.15 \pm 0.04 & [37] \\ 0.15 \pm 0.06 & [38] \\ 0.20 \pm 0.03 & [*] \end{cases}$$

$$^3S_1 \; : \; \frac{BR(p\bar{p} \to K^*(892)\bar{K})_{I=1}}{BR(p\bar{p} \to K^*(892)\bar{K})_{I=0}} \; = \; \begin{cases} 14 \pm 8 & [37] \\ 3.7 \pm 1.1 & [38] \\ 4.9 \pm 0.5 & [*] \end{cases}$$

Our coupled-channel analysis fits the $K^+K^-\pi^0$ and $K^\pm K^0\pi^\mp$ Dalitz-plots by means of the same production parameters [3] so that the previous ratios can be evaluated also in $K^+K^-\pi^0$ final state

$$\frac{BR(p\bar{p} \to K^*(892)\bar{K})_{I=1}}{BR(p\bar{p} \to K^*(892)\bar{K})_{I=0}} \; = \; \begin{cases} 0.33 \pm 0.06 & ^1S_0 \\ 7.8 \pm 0.7 & ^3S_1 \end{cases}$$

Contrary to $K^\pm K^0\pi^\mp$, in this final state both isospin sources have the same interference pattern between $K^{*+}K^-$ and $K^{*-}K^+$ intermediate states, so that the previous ratio is exactly the ratio of the $I = 1$ and $I = 0$ $K^*\bar{K}$ production processes.

The observed suppression of $K^*(892)\bar{K}$ production from $^3S_1$ $I = 0$ partial wave is connected to the related $K\bar{K}$ production. The isospin decomposition leads to the following expression of the ratio of branching ratios: $BR(p\bar{p} \to K^+K^-)/\, BR(p\bar{p} \to K^0\bar{K}^0) = |A_0 + A_1|/|A_0 - A_1|$, where A_0 and A_1 are the amplitudes of the process corresponding to $I = 0$ and $I = 1$ respectively. Experimentally [43] the ratio in $^3S_1$ turns out to be of the order of one, requiring one of the two isospin amplitudes to be negligible. The measurements of $BR(\bar{n}p \to K^+\bar{K}^0_S)$ [29] and $BR(\bar{p}d \to K^0K^-p)$ [30], whose values are comparable to the $BR(p\bar{p} \to K^+K^-)$ branching ratio, lead to the conclusion that the $I = 1$ amplitude dominates $K\bar{K}$ production from $^3S_1$ partial wave.

The availability of experimental data at different densities gives access for the first time to the investigation of P–wave annihilation where we get the following results in the $K^\pm K^0\pi^\mp$ final state:

$$\frac{BR(p\bar{p} \to K^*(892)\bar{K})_{I=1}}{BR(p\bar{p} \to K^*(892)\bar{K})_{I=0}} \; = \; \begin{cases} 0.24 \pm 0.03 & ^1P_1 \\ 0.092 \pm 0.015 & ^3P_1 \\ 3.9 \pm 0.4 & ^3P_2 \end{cases}$$

and in the $K^+K^-\pi^0$ final state:

$$\frac{BR(p\bar{p} \to K^*(892)\bar{K})_{I=1}}{BR(p\bar{p} \to K^*(892)\bar{K})_{I=0}} \; = \; \begin{cases} 0.34 \pm 0.03 & ^1P_1 \\ 0.12 \pm 0.02 & ^3P_1 \\ 5.9 \pm 0.4 & ^3P_2 \end{cases}$$

The suppression of one of the two allowed isospin components which operates in S–wave works also in P–wave annihilation. Despite this fact, while in S–waves the active isospin component has always positive G–parity, in P–waves this simple rule is not confirmed. In fact we get the following pattern of the dominant isospin components: $^1S_0$, $I = 0$; $^3S_1$, $I = 1$; $^1P_1$, $I = 0$; $^3P_1$, $I = 0$; $^3P_2$, $I = 1$.

$\rho(770)\pi$. The present determination of the $\rho(770)$ π QTB branching ratio (see Table 1) can be compared to $(59 \pm 3) \times 10^{-3}$ [45] in LH and to $(29.4 \pm 3.3) \times 10^{-3}$ [39] in NP hydrogen. Other determinations, obtained without a specific spin-parity analysis in our opinion are less reliable and will not be quoted. The fact that the $\rho(770)\pi$ channel branching ratio from $^3S_1$ $I = 0$ partial wave dominates largely the $^1S_0$ $I = 1$, is one of the most interesting and clearly established dynamical selection rule operating in $N\bar{N}$ annihilation ('$\rho\pi$ puzzle'). The relative strength of these sources is evaluated in our case using the QTB hadronic branching ratios (indicated by [*]), while, in the previous measurements, the ratios of branching ratios in LH from $^3S_1$ (divided by 3) and $^1S_0$ are used:

$$\frac{BR(p\bar{p} \to \rho(770)\pi, ^3S_1, I = 0)}{BR(p\bar{p} \to \rho(770)\pi, ^1S_0, I = 1)} \; = \; \begin{cases} > 13.8 & [45] \\ 17 \pm 7 & [39] \\ 12.4 \pm 1.2 & [46] \\ 12.7 \pm 1.6 & [*] \end{cases}$$

No '$\rho\pi$ puzzle' exists from P–wave annihilation where all partial waves contribute in a balanced way as shown in Table 4. Nevertheless something unexpected happens in the $^1P_1$ partial wave where the $\rho(770)\pi$ production with relative angular momentum $L = 2$ dominates the $L = 0$ component. This effect is clearly seen just by looking at the experimental data. In the first row of Fig. 1 are represented the slices of $\pi^+\pi^-\pi^0$ Dalitz-plots under the $\rho^0(770)$ peak. These give the outline of the neutral $\rho(770)$ crest, which can be produced only from $^3S_1$ and $^1P_1$ partial waves. The two big peaks are generated by the interference of neutral and charged $\rho(770)$ signals. In the second row are represented the projections, in the same invariant mass position, of the

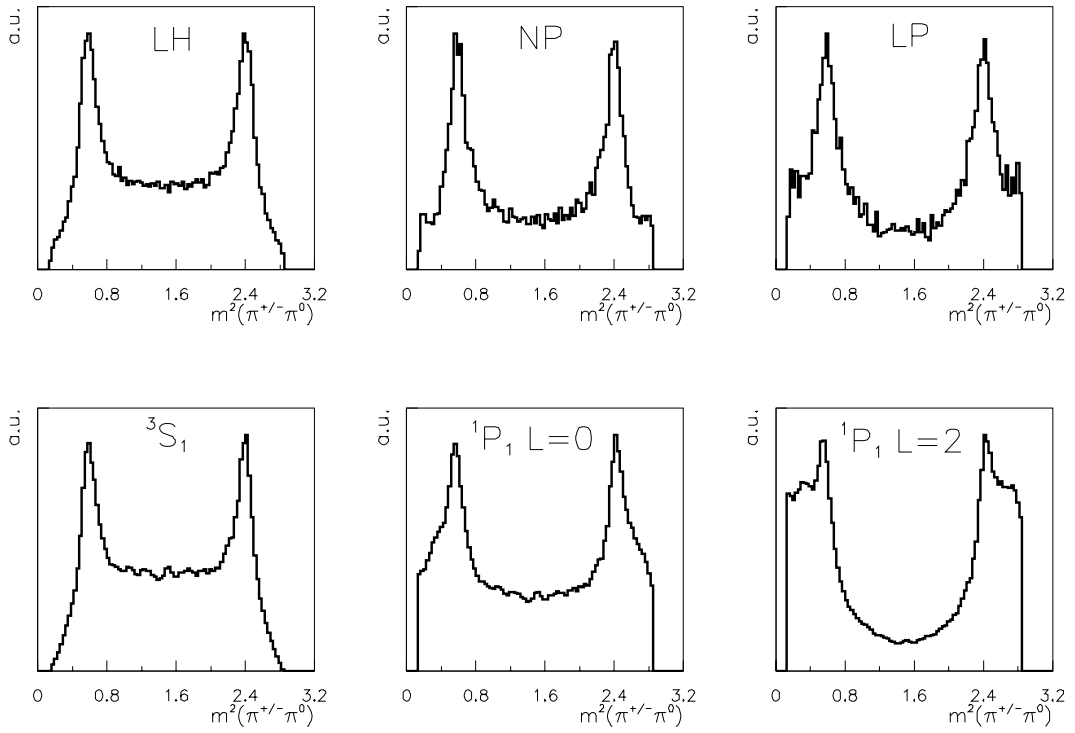

Fig. 1. Contour of the event distribution under the $\rho^0(770)$ peak in $\bar{p}p \to \pi^+\pi^-\pi^0$ at LH, NP, and LP (first row). Contour of $\rho^0(770)$ distribution from the single partial waves and angular momentum $^3S_1$, $^1P_1$ $L = 0$, and $^1P_1$ $L = 2$ (second row)

$^3S_1$, $^1P_1$ $L = 0$ and $^1P_1$ $L = 2$ partial waves. It is clear that in liquid hydrogen the shape of the experimental data is essentially controlled by the $^3S_1$ production. By lowering the hydrogen density, two little narrow peaks appear at the edge of the distribution. This characteristic shape, located around the $\rho^0(770)$ peak, can be produced only by the $L = 2$ component of the $^1P_1$ partial wave.

$f_2(1270)\pi$. Due to the fact that $f_2(1270)$ resonance is observed in $\pi\pi$ and $K\bar{K}$ decay mode, the $f_2(1270)\pi$ QTB branching ratio at different densities can be determined from $\pi^+\pi^-\pi^0$ and $K^+K^-\pi^0$ final states. The values obtained agree within the experimental errors (see Table 1). The liquid hydrogen determination can be compared to $(4.3 \pm 1.2) \times 10^{-3}$ ($\pi^+\pi^-\pi^0$ final state [45]), $\sim 6.4 \times 10^{-3}$ ($\pi^0\pi^0\pi^0$ final state [26]), $(3.1 \pm 1.1) \times 10^{-3}$ ($\pi^0\pi^0\pi^0$ final state [31]) and $(3.7 \pm 0.5) \times 10^{-3}$ ($K_LK_L\pi^0$ final state [47]). Of these values, only the second is obtained in the frame of a spin-parity analysis which includes P–waves in liquid hydrogen as it was done in our analysis. Measurements at different densities in $\pi^+\pi^-\pi^0$ are obtained in [46] (LH:$(8.5 \pm 0.6) \times 10^{-3}$; NP:$(12.0 \pm 0.9) \times 10^{-3}$; LP:$(13.7 \pm 1.3) \times 10^{-3}$), these values agree, within the experimental errors, with the present determination. No particular dynamical selection rule seems to operate in this case due to the fact that the significant $f_2(1270)\pi$ production takes place from all the allowed partial waves (see Table 4).

$f_2'(1525)\pi$. Previous measurements of $f_2'(1525)\pi$ QTB branching ratio in LH can be found in the $K_LK_L\pi^0$ final state $(0.075 \pm 0.012) \times 10^{-3}$ [47] where pure S–wave annihilation is assumed and in the $K^+K^-\pi^0$ final state from $^1S_0$ in LH $(0.226 \pm 0.068) \times 10^{-3}$ [21]. The strong disagreement of the first value with the OBELIX determination, could be due to the assumption made in [47] of pure S–wave annihilation in LH which is, in our opinion, a too drastic approximation. Concerning LP hydrogen, the measurement of the $f_2'(1525)\pi$ production from P–waves is $(2.04 \pm 0.20) \times 10^{-3}$ [21], to be compared with our determination obtained by subtracting S–wave contribution in LP branching ratio (Table 1) $(0.43 \pm 0.07) \times 10^{-3}$. These values are not compatible, but the following remarks are necessary.

When [21] was published, the $f_J(1710)$ spin was not clearly established so that both spin 0 and 2 hypothesis was tested. Due to a marginal χ^2 improvement ($\chi^2 = 2.06$ against $\chi^2 = 2.04$) the spin 2 was preferred and the quoted P–wave $f_2'(1525)\pi$ branching ratio was given. For the sake of completeness also the spin 0 hypothesis was explored obtaining values ranging from $(0.48 \pm 0.19)10^{-3}$ up to $(1.24 \pm 0.16)10^{-3}$. In the last years evidences in favour of the spin 0 hypothesis have been accumulated [5] so that we are forced to accept lower values of the $f_2'(1525)\pi$ P–wave branching ratios, which agree approximately with the present determination.

The ratio of $f_2'(1525)\pi$ and $f_2(1270)\pi$ hadronic branching ratios can be used to test possible OZI-rule violation effects in tensor mesons. From Table 4 we get the following values:

$$\frac{BR(p\bar{p} \to f_2'(1525)\pi)}{BR(p\bar{p} \to f_2(1270)\pi)} = \begin{cases} (37 \pm 5) \times 10^{-3} & ^1S_0 \\ (27 \pm 3) \times 10^{-3} & ^3P_1 \\ (52 \pm 13) \times 10^{-3} & ^3P_2 \end{cases}$$

to be compared to the OZI-rule theoretical expectation $R_{th} = \rho_{f_2'}/\rho_{f_2} \times tan^2(\theta_{2^{++}} - \theta_{id}) = 22 \times 10^{-3}$ ($\theta_{2^{++}} = 28^o$ [5]). These values seem not to require OZI-rule violation effects, neither in S nor in P–waves.

$a_2(1320)\pi$. In our analysis the $a_2(1320)$ is observed in $K^+K^-\pi^0$ and $K^\pm K^0\pi^\mp$ final states from different partial wave sources, so that the total branching ratios are different. The LH measurement in the $K^+K^-\pi^0$ final state can be compared only to $(15.6 \pm 1.8) \times 10^{-3}$ [47], while in $K^\pm K^0\pi^\mp$ final state the following value was published $(19.6 \pm 2.1) \times 10^{-3}$ [49], in agreement with our determination. The branching ratios in LH from $^1S_0$ and $^3S_1$ partial waves are also available $(19.9 \pm 5.5) \times 10^{-3}$ $(4.5 \pm 1.8) \times 10^{-3}$ [37] and $(24.4 \pm 3.7) \times 10^{-3}$ $(5.8 \pm 1.8) \times 10^{-3}$ [38] and can be compared to our determinations listed in Table 1.

The $a_2(1320)\pi$ production from the $^1S_0$ $I = 0$ partial wave dominates largely the $^3S_1$ $I = 1$ ('$a_2\pi$ puzzle'). Here the relative strength of these sources are evaluated using the hadronic branching ratios (indicated by [*]), while in the previous measurements the LH branching ratio values from $^3S_1$ (divided by 3) and $^1S_0$ were used

$$\frac{BR(p\bar{p} \to a_2(1320)\pi, ^1S_0, I = 0)}{BR(p\bar{p} \to a_2(1320)\pi, ^3S_1, I = 1)} = \begin{cases} 13 \pm 7 & [37] \\ 21 \pm 12 & [50] \\ 13 \pm 4 & [38] \\ 10.0 \pm 1.6 & [*] \end{cases}$$

The hadronic branching ratios in Table 4 indicate that the $^1S_0$ $I = 0$ dominate also over all P–waves. Moreover among P–waves, the enhanced $^1P_1$ contribution is observed.

4 Discussion of the results

As discussed in the previous Section, the present experimental data clearly indicate the complete suppression of $\phi(1020)\pi$ production from P–waves. Let's concentrate on this aspect by comparing the $\phi(1020)\pi$ (Table 1) and $\phi(1020)\eta$ [34] production branching ratios from $^1P_1$ partial wave obtained in LP hydrogen

$$BR(p\bar{p} \to \phi(1020)\,\pi) =< 0.1 \times 10^{-4} \qquad ^1P_1\ I = 1$$
$$BR(p\bar{p} \to \phi(1020)\,\eta) = (1.55 \pm 0.35) \times 10^{-4}\ ^1P_1\ I = 0.$$

These values suggest that the $^1P_1$ $\phi(1020)\pi$ suppression has not a kinematical origin, since it cannot be explained by means of phase space correction which is $\sim 30\%$. This effect is probably related to some mechanism which favours the $\phi(1020)$ production from the $^1P_1$ $I = 0$ partial wave of $p\bar{p}$. The same branching ratios from $^3S_1$ in LH (see Table 1 and [34] respectively) assume the following values:

$$BR(p\bar{p} \to \phi(1020)\,\pi) = (6.0 \pm 1.7) \times 10^{-4} \qquad ^3S_1\ I = 1$$
$$BR(p\bar{p} \to \phi(1020)\,\eta) = (0.49 \pm 0.02) \times 10^{-4}\ ^3S_1\ I = 0$$

which are compatible with the existence of a mechanism which enhances the $\phi(1020)$ production from the $^3S_1$ $I = 1$ $p\bar{p}$ partial wave. It is really remarkable that, in each partial wave, the dominant $p\bar{p}$ isospin in $\phi(1020)$ production coincides with the dominant $p\bar{p}$ isospin in the $K^*(892)\bar{K}$ production. This fact seems to be compatible with $K^*\bar{K}$ rescattering models [44] which attribute the large $\phi(1020)\pi$ production, i.e. the large apparent OZI-rule violation, to the rescattering between the $\bar{K}$ spectator and the K from $K^*(892)$ decay.

By assuming this point of view the general features of the dynamics involved in the annihilation process could be the following:

- a fraction of meson dynamics which takes place in $p\bar{p}$ annihilation is due to rescattering processes;
- in case the resonant states can be produced by $p\bar{p}$ system the rescattering contribution turns out to be masked from the direct production and, with the only limit of selection rules, all partial waves contribute to the production;
- in case the resonant state production from $p\bar{p}$ system is suppressed the rescattering contribution can dominate. In these cases, if rescattering process has some peculiar trend, it can be recognized by the inspection of the hadronic QTB branching ratios.

Following this scheme the $K^*(892)\bar{K}$ rescattering process, besides generating a large apparent OZI-rule violation, reflects its peculiar isospin pattern in the $\phi(1020)\pi$ production, since its direct production is strongly suppressed by OZI-rule. In this case, if we assume $\rho\pi\pi$ and K^*K rescattering contribution to $\phi\pi$ to be of the same magnitude [43], from Table 4 we can estimate the K^*K rescattering contribution from $^3S_1$ to be $\sim 12\%$.

Like the $\phi(1020)\pi$, also the $a_0(980)\pi$ P–wave production turns out to be suppressed, being produced abundantly from $^1S_0$, fairly from $^3P_1$ and negligibly from $^1P_1$. Also in this case the process seems to be driven by the $K^*(892)\bar{K}$ production. In fact the comparison of $a_0(980)\pi$ (Table 1) and $a_0(980)\eta$ [31] branching ratios from $^1S_0$ LH

$$BR(p\bar{p} \to a_0(980)\,\pi) = (30 \pm 3) \times 10^{-4} \qquad ^1S_0\ I = 0$$
$$BR(p\bar{p} \to a_0(980)\,\eta) = (2.2 \pm 0.7) \times 10^{-4}\ ^1S_0\ I = 1$$

suggests a strong dominance of $^1S_0$ $I = 0$ partial wave in the $a_0(980)$ production (that also in this case cannot be explained by means of phase space correction which is $\sim 30\%$), while the low $^1P_1$ hadronic branching ratio agrees with the suppression of $^1P_1$ $I = 1$ $p\bar{p}$ source (in this case $a_0(980)\eta$ branching ratio is not available). At first sight this scheme cannot reconcile the low $^3P_1$ $I = 0$ hadronic branching ratio of the $a_0(980)\pi$ with the strong $K^*(892)\bar{K}$ production observed in this partial wave. In our opinion no definitive conclusion can be drawn since $K^*(892)\bar{K}$ is produced, with comparable hadronic branching ratios, in two different angular momentum configurations (see Table 4) which, in principle, can interfere destructively.

As in the case of the $\phi(1020)$ a question arises. What kind of mechanism suppresses the $a_0(980)$ direct production so that the peculiar pattern of rescattering processes, i.e. the $K^*(892)\bar{K}$ production, could be manifest? The idea that $a_0(980)$ could be a molecular state [40] produced by $K\bar{K}$ diffusion can explain this fact. Another possible interpretation is offered by the four–quark hypothesis which

assumes a $qs\bar{q}\bar{s}$ structure of $a_0(980)$ [41]. In fact, experimental data show the strong suppression of $qq\bar{q}\bar{q}$ states (the $I = 2$ signal in $\bar{n}p \to \pi^+\pi^-\pi^+$ is of the order of 3×10^{-3} of the total [42]) and suggest an even stronger suppression of four quarks $qs\bar{q}\bar{s}$ states, i.e. of the $a_0(980)$ production. The latter hypothesis agrees qualitatively also with the low hadronic branching ratios of $f_0(980)\pi$ from $^1S_0$ $I = 1$ and $^3P_1$ $I = 1$ partial waves. In fact, the four–quarks hypothesis requires a $qs\bar{q}\bar{s}$ structure also for $f_0(980)$ so that a production driven by $K^*(892)\bar{K}$ is expected also in this case. Taking into account that $K^*(892)\bar{K}$ $^1S_0$ $I = 1$ and $^3P_1$ $I = 1$ partial waves are suppressed we could explain the relatively low $f_0(980)\pi$ production.

Following the scheme so far discussed the peculiar behavior of $\phi(1020)$ and $a_0(980)$ (and also of $f_0(980)$) is traced back to the unexplained isospin dependence of $K^*(892)\bar{K}$ production, which assumes, in this way, a fundamental role. At this level the other remarkable dynamical selection rules operating in S–wave i.e. the enhancement of $\rho(770)\pi$ and $a_2(1320)\pi$ production from $^3S_1$ $I = 0$ and $^1S_0$ $I = 0$ respectively, turns out to be independent phenomena. The possibility of connecting these facts could arise only in a frame which relates the different resonances like the SU_3 coupling scheme proposed in [48].

5 Conclusions

The measurement of the annihilation reactions $\bar{p}p \to \pi^+$ π^- π^0, $K^+K^-\pi^0, K^\pm\pi^\mp K^0$ at rest in hydrogen targets of different densities give access for the first time to the systematic investigation of P–wave dynamics. In addition, the available two different isospin combinations of the $K\bar{K}\pi$ final state allow the reliable separation of $I = 0$ and $I = 1$ meson dynamics (i.e. f_0, a_0 and a_2 isobars) and the disentanglement of the interfering sources (the two isospin components of $\bar{p}p$ system) of the $K^*(892)K$ final state. In this way a decisive improvement in the analysis of this final state is obtained. The main results are the following.

Similar trends characterize the $f_2(1270)\pi$ and $f_2'(1525)$ π production where all the allowed partial waves contribute with comparable hadronic branching ratios. No relevant OZI-rule violation effects are involved both in S and P partial waves.

The strong dominance of $\phi(1020)\pi$ and $a_0(980)\pi$ production from the $p\bar{p}$ system S–waves is clearly exhibited by the experimental data and confirmed by the values of the hadronic branching ratios obtained by the fit. The comparison between $\phi(1020)\pi$ (Table 1) and $\phi(1020)\eta$ branching ratios [34] suggests a suppression mechanisms related to $p\bar{p}$ isospin confirmed also by $a_0(980)\pi$ (Table 1) and $a_0(980)\eta$ [31] branching ratios from $^1S_0$ liquid hydrogen (at present $a_0(980)\eta$ branching ratios from P–waves are not available).

For the first time the $K^*(892)\bar{K}$ production was observed from P–waves. The dominance of one of the two allowed $p\bar{p}$ isospin sources observed in S–wave works also in P–waves with comparable intensities ($^1S_0$, $I = 0$; $^3S_1$, $I = 1$; $^1P_1$, $I = 0$; $^3P_1$, $I = 0$; $^3P_2$, $I = 1$).

The remarkable coincidence between the dominant isospin sources of $K^*(892)\bar{K}$ and $\phi(1020)\pi$ suggests the important role of the rescattering processes in the final state dynamics [44] (this approach explains also the large $\phi(1020)\pi$ production in $p\bar{p}$ annihilation which determines the large apparent OZI-rule violation). If we enlarge this scheme to the $a_0(980)\pi$ production, which exhibits the same characteristics, a relevant part of the dynamical selection rules observed in S and P–wave from $p\bar{p}$ annihilation are traced back to the isospin dependence of $K^*(892)\bar{K}$ production which would assume in this way a fundamental role.

The $\rho(770)\pi$ and $a_2(1320)\pi$ production turns out to be strongly dominated by $^3S_1$ $I = 0$ and $^1S_0$ $I = 0$ partial waves respectively. The enhancement of these partial waves represents the second fundamental feature emerging from quasi two body $p\bar{p}$ annihilation. Contrary to the expectations we found that the largest part of $^1P_1$, $\rho(770)\pi$ signal is produced with relative angular momentum $L = 2$ instead of $L = 0$. This is an interesting example of a dynamical mechanism clearly related to the kinematics of the system.

This set of data shows clearly that selection rules of dynamical origin overlap the established SU_2 and SU_3 symmetries in modulating the production of quasi two body final states. Clear indications suggest that these dynamical selection rules operate at two different levels. In fact, some of these (like the $\phi(1020)\pi$ production), seem to be related simply to the rescattering of mesons in the final state and are not significant as fas as the dynamics of the annihilation process is concerned, while other, like the $K^*(892)\bar{K}$, $\rho(770)\pi$, $a_2(1320)\pi$ production seem to operate at a deeper level and are related to the quantum number of $p\bar{p}$ system. Most probably the latter are not independent (see for instance the SU_3 coupling scheme approach [48]) and could be basis for wider investigations.

References

1. S. Okubo, Phys. Lett. B **5**, 165 (1963); G. Zweig, CERN Report no. 8419/th 412 (1964); I. Izuka, Prog. Theor. Phys. (suppl 37) **38** 21 (1966)
2. C.B. Dover, T. Gutsche, M. Maruyama, A. Faessler Prog. Part. Nucl. Phys. **29**, 87 (1992)
3. M. Bargiotti et al., Eur. Phys. Jour. C **26**, 371 (2003); Phys. Lett. B **561**, 233 (2003)
4. M. Bargiotti et al., EPJdirect A **2**, 1 (2002)
5. Review of Particle Physics, Phys. Rev. D **66**, 010001 (2002)
6. C.J. Batty, Nucl. Phys. A **601**, 425 (1996)
7. P. Salvini, G. Bendiscioli, A. Fontana, P. Montagna, Nucl. Phys. A **696**, 527 (2001)
8. V.G. Ableev et al., Phys. Lett. B **329**, 407 (1994)
9. M. Doser et al., Nucl. Phys. A **486**, 493 (1988)
10. M. Bargiotti et al., Phys. Rev. D **25**, 12001 (2002)
11. M. Agnello et al., Phys. Lett. B **337**, 226 (1994)
12. C. Amsler et al., Phys. Lett. B **297**, 214 (1992)
13. M. Bargiotti et al., Phys. Rev. D **65**, 0120011 (2002)
14. A. Zoccoli, Yad. Fiz. **59** 1448 (1996)
15. C. Amsler et al., Z. Phys. C **58**, 175 (1993)
16. L. Adiels et al., Z. Phys. C **42**, 49 (1989)
17. C. Amsler et al., Z. Phys. C **58**, 175 (1987)
18. A. Bertin et al., Phys. Lett. B **386**, 486 (1996)

19. M. Doser et al., Phys. Lett. B **215**, 792 (1988)
20. A. Bertin et al., Phys. Lett. B **385**, 493 (1996)
21. V. Alberico et al., Phys. Lett. B **438**, 430 (1998)
22. P. Salvini et al., submitted to Eur. Phys. Jour. C , (2003)
23. M. Doser et al., Phys. Lett. B **215**, 792 (1988)
24. G. Bendiscioli et al., Nucl. Phys. A **686**, 317 (2001)
25. U. Gastaldi et al., Phys. Lett. B **320**, 193 (1994)
26. C. Amsler et al., Phys. Lett. B **355**, 425 (1995)
27. A. Abele et al., Phys. Rev. D **57**, 3860 (1998)
28. M.G.Sapozhnikov, Phys. of Atomic Nuclei **62**, 1987 (1999)
29. A. Bertin et al., Phys. Lett. B **410**, 344 (1997)
30. A. Abele et al., Eur. Phys. Jour. C **17**, 583 (2000)
31. C. Amsler et al., Rev. Mod. Phys. **70**, 1293 (1998)
32. J. Reifenrother et al., Phys. Lett. B **267**, 299 (1991)
33. V.G. Ableev et al., Nucl. Phys. A **594**, 375 (1995)
34. V. Alberico et al., Phys. Lett. B **432**, 427 (1998)
35. A. Bertin et al., Phys. Lett. B **434**, 180 (1998)
36. PhD. Thesis of M. Heinzelmann (1996)
37. B. Conforto et al., Nucl. Phys. B **3**, 495 (1967)
38. A. Abele et al., Phys. Rev. D **57**, 3860 (1998)
39. B. May Z. Phys. C **46**, 191 (1990)
40. Review of particle physics, Phys. Rev. D **66**, 010001-754 (2002)
41. M. Alford, R.L. Jaffe hep-lat/0001023; hep-lat/0306037
42. A. Filippi et al., Phys. Lett. B **495**, 284 (2000); Nucl. Phys. A **692**, 287 (2001)
43. E. Klempt, Phys. of Atomic Nuclei **57**, 1565 (1994)
44. V.E. Markushin, Nucl. Phys. A **655**, 185 (1999); D. Buzatu, F.M. Lev, Phys. Part. Nucl. **29**, 88 (1998); A.V. Anisovich, E. Klempt, Z. Phys. A **354**, 197 (1996); M.P. Locher, Yang Lu, Z. Phys. A **351**, 83 (1995)
45. M. Foster et al., Nucl. Phys. B **6**, 107 (1968)
46. A. Bertin et al., Phys. Lett. B **408**, 476 (1997)
47. A. Abele et al., Phys. Lett. B **385**, 425 (1996)
48. E. Klempt et al., Z. Phys. A **354**, 67 (1996)
49. R. Armenteros et al. CERN-PRE-86-053
50. P. Espigat et al., Nucl. Phys. B **36**, 93 (1972)